

Table of Contents

Source Protection Explorer – Data and Methods	3
1 City Water Map	3
1.1 City selection	3
1.2 Intake data collection	3
1.3 Mapping intake points	3
2 Pollution yield and pollution reduction potential	3
2.1 Identifying contributing areas	3
2.2 Estimating sediment and phosphorus yields	4
2.3 Sediment and phosphorus reduction potential	4
2.4 Modeling conservation activities	4
2.5 Estimating baseline loading	4
2.6 Calculating pollution yields and reduction potential	5
2.7 Analysis outputs	5
3 Conservation costs	
3.1 Costs of conservation implementation	6
3.2 Per capita implementation costs	6
Benefits Explorer – Data and Methods	8
1 Global map of urban source watersheds	
2 Climate Change Mitigation	11
2.1 Standing forest carbon	
2.2 Forest loss	
2.3 Reforestation potential	
3 Biodiversity	
3.1 Imperiled terrestrial species	
3.2 Freshwater Biodiversity Threat Index	
4 Human Health & Well-Being	
4.1 Impact of pollination loss on crop and micronutrient production and the	
cost	

4.2 Total annual excess nitrogen application	16
5 Additional Data	18
5.1 Proportion of unprotected natural land cover within source watersheds needed to meet Aichi Biodiversity Target 11	18
5.2 Reducing regional species extinction risk	19
5.3 Rarity-weighted richness of freshwater and terrestrial ecoregions	21
Water Funds Explorer	23
Water Scarcity Explorer – Data and Methods	25
1 Time Series of irrigation depletion	25
2 Water Scarcity Condition Categories	25

Source Protection Explorer – Data and Methods

1 City Water Map

1.1 City selection

This analysis builds upon The Nature Conservancy's previous work characterizing water risks and opportunities for cities around the world.^{1–3} Briefly, data on cities and their water sources were collected in three phases. In the first phase, data was collected for the 50 largest cities by population. In the second phase, a stratified sample was identified for cities populations ranging from less than one million to more than 5 million. Finally, data was collected from easily sources for cities in the United States, as well as additional data for specific cities relevant to partner organizations.

1.2 Intake data collection

For each city in our sample we consulted a variety of data sources to collect information about water supplies. Where possible we utilized official government or water utility publications as primary data sources. When such data sources were not readily accessible or provided incomplete data other sources were consulted, including personal communications, academic literature, periodicals and general internet searches. Additionally, the collected data was typically compared against multiple sources as further verification. Information on source names, source types and suppliers were, in general, readily identified. Other information, including intake coordinates and diversion volumes, were more difficult to establish. In some cases, we had to use data sources of lower certainty, such as the website of the water utility or official press releases, which often listed water sources. Once the place names of water sources were identified, we geo-located the sources. Unique place names were identified using Google Earth or other geographical atlases. In some cases, a text description of a source (e.g., "three miles upstream of the city along the same river that flows through the city") was mapped in a geographical information system (ArcGIS 10.2).

1.3 Mapping intake points

The locations of surface freshwater withdrawal points were adjusted ("snapped") to match the underlying hydrographic river system; in this case these are represented by the global high resolution hydrographic dataset HydroSHEDS.⁴ If the snapping adjustment step is not performed small spatial errors in the location of a point could lead to large errors in the estimation of the available water. First, we selected withdrawal points within 10 kilometers of the coast and manually adjusted their location to ensure that, in the underlying hydrographic system, they were not falling on areas that are considered saline water. Second, for withdrawal points on lakes we adjusted the location to be at the outflow of the lake, defined as the lowest point of the lake feature in a global database of lakes, reservoirs and wetlands (GLWD). This correction allowed the catchment of the lake and its corresponding water availability to be correctly derived. Finally, using the Snap Pour Point command in ArcGIS, we adjusted the location of withdrawal up to five cells (2.5 kilometers) to match the point of greatest flow accumulation.

2 Pollution yield and pollution reduction potential

2.1 Identifying contributing areas

Sediment and nutrient loads were estimated for a set of pre-defined polygons delineating a globally-consistent set of watershed boundaries. This set of watershed boundaries was derived

using the HydroBASINS data set, which defines a hierarchical classification of sub-basin delineations globally.⁵ For any given point location within the spatial coverage of the HydroBASINS data set, the enclosing sub-basin and its upstream contributing sub-basins can then be identified.

For each of the intake points mapped previously using the City Water Map, we selected the enclosing HydroBASINS sub-basin (Level 12) and all upstream contributing sub-basins. We then define these HydroBASINS-delineated areas as the contributing area for a given intake point. It is important to note that these contributing areas differ from watershed boundaries that might be delineated using a digital elevation map (DEM). Particularly for small watersheds (less than ~100 km²), this discrepancy can be significant.

2.2 Estimating sediment and phosphorus yields

Information on sediment and nutrient loading was developed previously by the Conservancy and adapted more recently as part of a web application.^{2,3} Briefly, sediment loading was estimated using the Universal Soil Loss Equation (USLE). Data sources, input factors and approach followed those reported previously.² Phosphorus loading was estimated using an export coefficient approach, where each land-cover type exports a certain amount of nitrogen or phosphorus from a given pixel. In practice, nitrogen and phosphorus export are highly correlated at large scales and we report here values for phosphorus. The approach for export coefficient and nutrient application rates also followed those reported previously.² For both sediment and phosphorus, loading values were adjusted to estimated yields using information on contributing area size and distance from intake, calibrated using empirical models (SPARROW) developed by USGS for large basins in the United States.⁶

Additional details on the methodology for estimating sediment and phosphorus yields can be found in documentation for the *Urban Water Blueprint* or the Watershed Screening Tool (watershedtool.org).^{2, 3}

2.3 Sediment and phosphorus reduction potential

To assess the potential for realizing water quality benefits resulting from source watershed protection activities, we use an approach similar to that described previously.² For each watershed in our dataset, we identify the cost-optimal conservation area required to achieve a given pollution reduction target (e.g., the cost of achieving a 10 percent reduction in sediment). Then, we aggregate these watershed-level results to obtain global estimates of the total conservation action required to achieve these targets.

2.4 Modeling conservation activities

Previously, the Conservancy reported on the potential for certain types of source water protection activities to reduce the sediment and phosphorus pollution in watersheds.² Here, we extend this approach to consider the potential for a subset of activities to reduce sediment or phosphorus concurrently. We consider the reduction potential for three categories of land-based conservation activities: forest protection, pastureland reforestation and agricultural BMPs (modeled as cover crops).

2.5 Estimating baseline loading

Estimates of sediment and phosphorus loading follow the approach described above. Importantly, forest protection concerns mitigation of future risk. In order to facilitate comparative equivalency of reduction potential across all three activity types, we utilized a single modified estimate of baseline sediment and nutrient loading that incorporates estimates of the future risk of forest loss. Briefly, future loading for forest cover land types is assumed to be a

function of both loading and the probability of forest loss, where deforestation probabilities were estimated from changes in forest cover at the scale of biomes (using the time-incremented, land-cover datasets, GlobCover).⁷ In all cases, the deforestation pathway is assumed to result in a transition to pastureland.

2.6 Calculating pollution yields and reduction potential

Using these loading estimates for each watershed within our global map of urban source watersheds, the predicted yields of sediment and phosphorus are derived at the watershed outlet. Predicted yields are obtained from the Watershed Conservation Screening Tool which uses an approach adapted from McDonald and Shemie. The data utilized here in this analysis incorporate revisions that were later used in the Watershed Conservation Screening Tool (watershedtool.org), which include additional model refinements to further improve the calculation of predicted yields. In addition to accounting for overland attenuation of pollutants as done previously, the Screening Tool further accounts for instream attenuation of pollutants. This modification is expected to further improve predictive accuracy, particularly for large watersheds where instream attenuation can be significant. Model parameters were calibrated against measured water quality data collected for watersheds in the United States, as described in the Screening Tool documentation.

With estimates of predicted yields under baseline conditions and under implementation of the three source water protection activity types, we calculate the reduction potential for all relevant pixels for each practice type across a given watershed. This results in a curvilinear range of reduction values across a given watershed, with some pixels holding greater potential to reduce sediment or nutrient yields per unit area. We subsequently convert these curves to marginal costs curves using information obtained previously on estimated implementation costs across activity types and regions. Finally, we use simple one-dimensional optimization to identify the optimal marginal cost at which a given reduction target can be achieved.

2.7 Analysis outputs

The primary output of this analysis is an estimate for each source watershed within our data set of the conservation implementation area needed to achieve a given pollution reduction target. For each watershed and each reduction target (e.g., 10 percent reduction in sediment), we derive values for the total area of implementation under forest protection, reforestation and agricultural BMPs. For some watersheds, the specified reduction target may not be achievable. In these instances, we do not record implementation area values, but we do include the spatial extent of these watersheds when determining the scope of potential.

For subsequent analyses, these activity area estimates are used to define possible implementation scenarios. For example, we estimate city-level costs and cost savings for achieving a 10 percent reduction in sediment or nutrients. It is important to note that such scenarios are necessarily limited in scope. Here, we optimize for a single parameter (implementation costs) alone. A more robust – and more socially relevant – optimization approach would consider multiple parameters. For this and other reasons, these results should be interpreted with discretion.

It is also important to note that this optimization is performed at the scale of watersheds. To derive global-level approximations from these watershed-level implementation scenarios, we incorporate conditional assumptions regarding implementation across these watersheds. Namely, given the non-spatial nature of our pollution yield estimates, we assume an equal probability of activity implementation across all relevant pixels for a given activity type. Where overlapping areas occur, we further assume implementation at the maximum area required for

that overlapping area. This results in an approximated global view of conservation activity implementation in order to reach or exceed the specified reduction target.

3 Conservation costs

3.1 Costs of conservation implementation

We estimate costs of conservation implementation utilizing regional estimates reported previously. Using our estimates of implementation area for each conservation practice type, we estimate total annual costs to achieve 10, 20, and 30 percent reduction in sediment or nutrients for each watershed in our data set. In many cases, a given reduction target cannot be reached and we report null values.

For cities with a single source watershed, we associate these watershed-level costs with the respective sourcing cities. For cities with multiple source watersheds, we first calculate the average implementation area for each practice type using the approach described previously. These average implementation area values are then used to derive representative cost values at the city level.

3.2 Per capita implementation costs

While total annual costs for conservation can be informative for assessing the feasibility of source protection implementation, such a measure does not account for the potential corresponding scale of benefits. As a proxy for such benefits, we calculate the costs of conservation relative to the city population that might benefit from such improvements in source water quality. City population estimates were derived from United Nations Population Division for the year 2005 as previously reported. To account for regional and national differences in currency purchasing power, we further normalize these per capita costs relative to national per capita GDP.8

References

- 1. McDonald, R.I., Weber, K., Padowski, J., et al., (2014). Water on an Urban Planet: Urbanization and the Reach of Urban Water Infrastructure. *Global Environmental Change* **27**: 96-105. doi: 10.1016/j.gloenvcha.2014.04.022
- 2. McDonald, R.I. and Shemie, D. (2014). Urban Water Blueprint: Mapping Conservation Solutions to the Global Water Challenge. The Nature Conservancy, Washington, D.C., USA. http://water.nature.org/waterblueprint
- 3. McDonald, R.I. (2016). EcoLogic--The Watershed Conservation Screening Tool: A Resource for Large Water Users. *Journal-American Water Works Association* **108**: 18-20. doi: 10.5942/jawwa.2016.108.0107
- 4. Lehner, B., Verdin, K., and Jarvis, A. (2008). New Global Hydrography Derived from Spaceborne Elevation Data. *Eos, Transactions, American Geophysical Union* **89**: 93-94. doi: 10.1029/eost2008EO10
- 5. Lehner, B. and Grill, G. (2013). Global River Hydrography and Network Routing: Baseline Data and New Approaches to Study the World's Large River Systems. *Hydrological Processes* **27**: 2171–2186. doi: 10.1002/hyp.9740
- 6. USGS. (2016). USGS SPARROW Surface Water-Quality Modeling. Available from https://water.usgs.gov/nawqa/sparrow/index.html. (Accessed: 11th January 2017)
- 7. Arino, O., Ramos Perez, J.J., Kalogirou, V., Bontemps, S., Defourny, P., Van Bogaert, E. (2012). Global Land Cover Map for 2009 (GlobCover 2009). European Space Agency (ESA)

and Université catholique de Louvain (UCL). Available from http://due.esrin.esa.int/page_globcover.php (accessed July 2016). doi:10.1594/PANGAEA.787668

8. The World Bank. (2016). World Development Indicators, 1960-2016. *World Bank Open Data Catalog*. Available from http://data.worldbank.org/. (Accessed: 1st August 2016)

Benefits Explorer – Data and Methods

1 Global map of urban source watersheds

Data

There are four main data sources used to identify source watershed areas: hydrological data, global city data, surface water withdrawal locations for cities and HydroBASIN-derived modeling data.

Hydrological data comprises the flow direction, flow accumulation (i.e., watershed size) and discharge grids provided by the HydroSHEDS database at 15 arc-second (approx. 500 meters at the equator) pixel resolution (Lehner and Grill 2013). All watershed boundaries were calculated from this data.

The second data source comprises the global city locations and population numbers taken from the Global Rural-Urban Mapping Project (GRUMP), obtained from the Center for International Earth Science Information Network (CIESIN et al. 2011). The original vector data contains 67,935 points representing cities recorded with various attributes, including population estimates, valid as of the year 2000.

The third data source comprises the water intake locations for cities obtained from The Nature Conservancy's Urban Water Blueprint (UWB) project and its underpinning City Water Map (CWM) (McDonald et al. 2014). This dataset originally contained 471 global cities with 1,505 unique intake locations.

The final data source comprises information on HydroBASIN-derived watersheds from source watershed protection models. The Watershed Conservation Screening Tool models non-atmospheric nonpoint sediment and nutrient (phosphorus) yields, and the potential for selected conservation practices to reduce these yields. This dataset includes more than 1 million watersheds with at least partial coverage across all continents (excluding Antarctica).

Importantly, these data sources focus only on potential surface water sources for cities. These data and related analyses do not consider implications of other water sources, most notably groundwater.

Methodology

City selection criteria

All cities of the world with a reported population of at least 100,000 people in the GRUMP database were used. Additionally, we used all CWM cities with surface water intakes and their intake locations.

City Water Map cities

The database of the City Water Map (CWM) originally contained 471 cities with 1,505 intake locations. The point locations of CWM intake points represent manually assigned withdrawal points that were snapped to the HydroSHEDS river network. However, 12 locations did not have data on withdrawal points or city names and were thus removed, resulting in 1,493 unique withdrawal locations.

GRUMP cities

The global GRUMP data used in this project also contained the same cities and suburbs of the urban agglomerations included in the CWM. These duplicated cities were manually identified and removed in order to eliminate double-counting of cities. After applying the 100,000-population threshold and removing the duplicate cities, 3,724 cities remained.

For all GRUMP cities, the precise water intake location was not known. In order to estimate most likely locations, two criteria were postulated: 1) that cities generally draw water from the largest river nearby; and 2) that larger cities have more capacity and size to reach further out. In order to simulate these criteria, the GRUMP cities were separated into three groups based on population size and then snapped to the highest flow accumulation value (i.e., the largest watershed size as given in the HydroSHEDS database) within a size-dependent distance (see Table 1). The snapped points were then assumed to represent the water intake locations of the GRUMP cities.

Table 1.1. Snapping distances for the GRUMP city locations

Population	Snapping Distance (decimal degrees)
100,000 - 500,000	0.10 (~10 km)
500,000 - 1,000,000	0.15 (~15 km)
> 1,000,000	0.20 (~20 km)

Combined CWM and GRUMP intakes

The snapped GRUMP points (3,724) and UWB withdrawal points (1,493) were then combined to create the final combined layer of potential intakes, containing 5,217 points. If two points were located within the same pixel of the HydroSHEDS flow direction grid, the point with the higher identifier was shifted one pixel downstream.

Final watershed layer

Each intake point was then mapped to its enclosing Level 12 HydroBASIN unit. For each of these HydroBASIN units, the Watershed Conservation Screening Tool has a corresponding polygon which includes all upstream HydroBASIN units. In this manner, each intake point is then associated with a corresponding polygon representing the entire upstream contributing area or watershed for that intake point. For all intake points, this HydroBASIN derived watershed differs in spatial extent from a watershed that might be derived using the precise intake point in conjunction with elevation data. These discrepancies are usually minor, but can be significant for smaller watersheds. Cities outside the spatial extent of the Screening Tool data set were excluded from subsequent analyses. The final watershed layer includes a total of 4,546 watersheds representing surface water sources for 4,138 cities.

References

Center for International Earth Science Information Network (CIESIN), Columbia University; International Food Policy Research Institute (IFPRI), the World Bank; and Centro Internacional de Agricultura Tropical (CIAT). (2011). Global Rural-Urban Mapping Project, Version 1 (GRUMPv1): Settlement Points. Socioeconomic Data and Applications Center (SEDAC), Columbia University, Palisades, New York. Available from http://sedac.ciesin.columbia.edu/data/dataset/grump-v1-settlement-points.

Lehner, B. and Grill, G. (2013). Global River Hydrography and Network Routing: Baseline Data and New Approaches to Study the World's Large River Systems. *Hydrological Processes* **27**: 2171–2186.

McDonald, R.I. (2016). EcoLogic--The Watershed Conservation Screening Tool: A Resource for Large Water Users. *Journal-American Water Works Association* **108**: 18-20.

McDonald, R.I., Weber, K., Padowski, J., et al., (2014). Water on an Urban Planet: Urbanization and the Reach of Urban Water Infrastructure. *Global Environmental Change* **27**: 96-105.

2 Climate Change Mitigation

2.1 Standing forest carbon

To visualize the distribution of pan-tropical, above-ground biomass stored in live woody vegetation, we summarized the total amount of above-ground carbon stored in all Level 5 HydroBASINS that intersect with our urban source watersheds. The primary data used to quantify above-ground biomass comes from a high resolution product that expands upon the methodology presented in Baccini et al. (2012) in order to generate a pan-tropical map of above-ground live woody biomass density at 30-meter resolution for the year 2000 (Baccini et al. *in review*; Zarin et al. 2016).

First, we calculated the total amount of above-ground biomass in live woody vegetation within the boundary of source watersheds that intersects with the tropical extent of the biomass data. We then converted the total estimate of above-ground biomass in our source watersheds into above-ground carbon using a conversion factor of 0.5 (IPCC 2003), since about 50 percent of plant biomass consists of carbon.

References

- Baccini, A., Goetz, S.J., Walker, W.S., et al., (2012). Estimated Carbon Dioxide Emissions from Tropical Deforestation Improved by Carbon-Density Maps. *Nature Climate Change* 2: 182-185.
- Baccini A., Walker, W., Carvahlo, L., Farina, M., Sulla-Menashe, D., and Houghton, R. (2015). Tropical Forests are a Net Carbon Source Based on New Measurements of Gain and Loss. In review. Accessed through *Global Forest Watch Climate: Summary of Methods and Data* on July 22nd, 2016. climate.globalforestwatch.org.
- IPCC. (2003). Good Practice Guidance for Land Use, Land-Use Change and Forestry. IPCC National Greenhouse Gas Inventories Programme, Hayama, Kanagawa, Japan. Available from http://www.ipcc-nggip.iges.or.jp/public/gpglulucf/gpglulucf_files/GPG_LULUCF_FULL.pdf (accessed July 2016).
- Zarin, D.J., Harris, N.L., Baccini, A., et al., (2016). Can Carbon Emissions from Tropical Deforestation Drop by 50% in 5 Years? *Global Change Biology* **22**: 1336-1347. doi: 10.1111/gcb.13153

2.2 Forest loss

We quantified the extent of forest loss in urban source watersheds using global-scale data from Hansen et al. (2013). We retrieved the global forest cover loss data from Google Earth Engine (GEE) and modified a Java-Script code by Tracewski et al. (2016) to conduct the analysis in GEE. We estimated tree cover in the year 2000 and tree cover loss between 2001 and 2014 with 30-meter cells from Landsat imagery. The original Hansen et al. (2013) data has been updated with years 2013 and 2014 on GEE using updated methodology.

For each Level 5 HydroBASIN unit that intersects with the urban source watersheds, we analyzed tree cover from the year 2000 and then calculated the total area of forest loss each subsequent year based on the year of loss. These years were summed to provide total square kilometers lost between 2001 and 2014 within each HydroBASIN.

These calculations assume that all original tree cover (based on the tree cover in the year 2000) within the pixel was lost. If the pixel's tree cover value in the year 2000 was 70 percent, then it was assumed that 70 percent of the pixel area lost forest in the year of forest loss (Tracewski et al. 2016). Each year of forest loss is mutually exclusive, meaning that forest loss can only occur in one pixel during one year.

In interpreting the results of this analysis, it is important to understand the definition of tree cover loss as it is defined by the algorithm used by Hansen et al. (2013) and that "loss" does not always equate to deforestation. Tree cover loss is identified by Hansen et al. in such a way that it includes anthropogenic causes of forest loss, including timber harvesting and deforestation, as well as natural causes such as disease. The dataset also identifies forest loss from fires that can start from both natural and human sources. Our analysis does not report forest cover gain, even though forests across source watersheds do experience variable rates of tree cover gain.

References

- Google Earth Engine Team. (2015). Google Earth Engine: A Planetary-Scale Geospatial Analysis Platform. https://earthengine.google.com
- Hansen, M.C., Potapov, P.V., Moore, R., Hancher, M., Turubanova, S.A., Tyukavina, A., Thau, D., Stehman, S.V., Goetz, S.J., Loveland, T.R., Kommareddy, A., Egorov, A., Chini, L., Justice, C.O., and Townshend, J.R.G. (2013). High-Resolution Global Maps of 21st-Century Forest Cover Change. *Science* **342**: 850–853. Data available online from: http://earthenginepartners.appspot.com/science-2013-global-forest.
- Tracewski, Ł., Butchart, S.H., Donald, P.F., Evans, M., Fishpool, L.D., and Graeme, M. (2016). Patterns of Twenty-First Century Forest Loss Across a Global Network of Important Sites for Biodiversity. *Remote Sensing in Ecology and Conservation* 2: 37-44. doi: 10.1002/rse2.13.

2.3 Reforestation potential

We used data derived from WRI's Atlas of Forest Landscape Restoration Opportunities (WRI 2014) to determine a reasonable estimate for the maximum area of reforestation opportunity per HydroBASIN intersecting the urban source watersheds. We applied two additional steps to extract only reforestation opportunities from WRI's data. First, we removed pixels located in grassland ecosystems using a spatially explicit dataset of global grassland types (Dixon et al. 2014). Then, we removed pixels of data that would not transition from a non-forested status to a forested status (here we define the transition from less than 25 percent tree cover to greater than 25 percent tree cover) (WRI 2014). Any of the reforestation and restoration opportunities that were not located within the boundaries of the urban source watersheds were removed from the analysis.

References

- Dixon, A.P., Faber-Langendoen, D., Josse, C., Morrison, J., and Loucks, C.J. (2014).
 Distribution Mapping of World Grassland Types. *Journal of Biogeography* **41**: 2003-2019. Doi: 10.1111/jbi.12381
- WRI. (2014). Atlas of Forest Landscape Restoration Opportunities. World Resources Institute, Washington, D.C., USA. Available from www.wri.org/forest-restoration-atlas.

3 Biodiversity

3.1 Imperiled terrestrial species

We quantified the number of imperiled terrestrial species that could benefit from source water protection activities within each HydroBASIN that intersects with the urban source watersheds. We used the spatial database for the IUCN Red List of Threatened Species to quantify the number of imperiled species that occur within urban source watersheds (BirdLife International and NatureServe 2015; IUCN 2016). Species were selected for the analysis if they had an IUCN code of critically endangered, endangered or vulnerable and if they are native or reintroduced and are extant to the region.

We incorporated birds, amphibians and terrestrial mammals into our analysis of terrestrial species. Additional criteria were applied to identify imperiled terrestrial species that could benefit from source water protection activities. We developed an approach that combined WRI's Atlas of Forest Landscape Restoration Opportunities (WRI 2014) with Oakleaf's (2016) Human Modification (HM) dataset, with the intention of restricting the count of species to places within urban source watersheds where source water protection activities could more realistically support their survival. We classified places within the urban source watershed region that have high human modification (HM values > 0.66) and that are not classified by WRI as reforestation or restoration opportunities as unsuitable habitat for source water protection activities to support the survival of imperiled terrestrial species. We assume that source water protection activities only support terrestrial species at the actual site of activity implementation.

We further restrict our count of imperiled terrestrial species within urban source watersheds to those species that have at least 10% of their range intersecting the suitable habitat mask. For migratory birds, the IUCN data includes migration distributions that are mapped across oceans. In the event that a bird migrates across the ocean, the 10-percent threshold only considered the species' terrestrial range.

References

BirdLife International and NatureServe. (2015). Bird Species Distribution Maps of the World. Version 5.0. BirdLife International, Cambridge, UK and NatureServe, Arlington, USA.

IUCN 2016. The IUCN Red List of Threatened Species. Version 2016-2. http://www.iucnredlist.org. Downloaded on 01 July 2016.

Oakleaf, J.R. (2016). Human Modification. Unpublished data. Retrieved from Jim Oakleaf, The Nature Conservancy (accessed July 2016).

WRI. (2014). Atlas of Forest Landscape Restoration Opportunities. World Resources Institute, Washington, D.C., USA. Available from www.wri.org/forest-restoration-atlas.

3.2 Freshwater Biodiversity Threat Index

We used data from Vörösmarty et al. (2010) (www.riverthreat.net) to examine levels of threat to freshwater biodiversity across the urban source watersheds. Vörösmarty et al. (2010) developed an incident index of freshwater biodiversity threat by combing various themes of impact, including catchment disturbance, pollution, water resource development and biotic factors. The incident values for the index of freshwater biodiversity threat are standardized and normalized between values 0 and 1. We summarized the HydroBASINS within our source watersheds by the

average biodiversity threat value. Vörösmarty et al. (2010) removed pixel values from the original data if they did not meet a minimum threshold of average annual runoff. If 20 percent of the HydroBASIN's area had insufficient data due to the minimum threshold of average annual runoff, we did not calculate the average index value of threat.

Reference

Vörösmarty, C.J., McIntyre, P.B., Gessner, M.O., Dudgeon, D., Prusevich, A., Green, P., Glidden, S., Bunn, S.E., Sullivan, C.A., Liermann, C.R., and Davies, P.M. (2010). Global Threats to Human Water Security and River Biodiversity. *Nature* **467**: 555-561. doi:10.1038/nature09440

4 Human Health & Well-Being

4.1 Impact of pollination loss on crop and micronutrient production and the agricultural opportunity cost

To characterize the impact of pollination services on agricultural value and micronutrient production, we used spatially explicit estimates of crop yield, hectares cultivated and country-specific prices. We used datasets on hectares in cultivation from Ramankutty et al. (2008) and crop yield from Monfreda et al. (2008). These datasets combined three sources of remotely-sensed land-cover data with a wide array of country- or county-specific agricultural census information to identify production and yield of 175 different crops for each 10-by-10 kilometer grid cell globally for the year 2000.

We combined the production and yield data with price information from the Food and Agricultural Organization of the United Nations (FAO 2016), multiplying the yield of each of the 175 crops by crop-specific prices for each of 250 national administrative units, measured in 2013 US dollars. When price information for 2013 was not available, we used the average price from all prior years that had price information for that crop in that country (inflation adjusted to 2013), or, failing that, the world average price for the crop.

Lack of pollinator habitat has a detrimental effect on the yield of pollination-dependent crops. We used data from Klein et al. (2007) to specify the proportion of yield that would be lost (calculated in dry-weight tons, at the farm gate) if pollination services were not available to agricultural production on each grid cell. The effect of pollination services on yield exhibits spatially heterogeneous effects with very localized impacts. As a result, we did not identify the relationship between specific source water protection activities and agricultural yield loss (the marginal value of protection), instead we characterized the total effect that pollination services offer. We summarized agricultural production with two scenarios: 1) a "baseline scenario" based on observed yields; and 2) a "reduced-pollination scenario" where crop yield was reduced by the respective pollination dependence.

To translate yield losses in these scenarios into nutritional effects, we followed the methodology of Chaplin-Kramer et al. (2014) to assign nutritional content information from the United States Department of Agriculture (2015) to each crop. We calculated the production of vitamin A under the baseline and reduced-pollination scenarios. We reported the average proportion of nutrient production that was lost for each source watershed.

To estimate the total agricultural economic value lost in the absence of pollination services, which we use as a proxy for the opportunity cost, we combined the high-resolution data (10-kilometer resolution) on crop production for 175 different crops (Monfred et al. 2008) with 2014 price information from the FAO for each crop. The prices used were specific to each FAO country to account for spatial heterogeneity of prices available. The total agricultural value in each grid cell of data is defined by the following equation:

$$\pi(h_{xy}) = \sum_{j=1}^{J} \sum_{i=1}^{I} p_{ij} * y_{i,xy}$$
 (1)

where p_{ij} is the crop- and country-specific price and $y_{i,xy}$ is the yield in dry-weight metric tons produced of crop i in the xy^{th} grid cell. If 2014 prices were not available for a country or crop, we used the average price from 2000 to 2013. If prices were not available at all for this time period, we used the continent average price.

References

- Chaplin-Kramer R., Dombeck E., Gerber J., Knuth K.A., Mueller N.D., Mueller M., Ziv G., Klein A.-M. (2014). Global Malnutrition Overlaps with Pollinator-Dependent Micronutrient Production. *Proceedings of the Royal Society B Biological Sciences* **281**: p.20141799. doi: 10.1098/rspb.2014.1799
- EarthStat. Cropland and Pasture Area in 2000. *EarthStat.org*, Global Landscapes Initiative, University of Minnesota and Ramankutty Lab, The University of British Columbia, Vancouver. Data available online from http://www.earthstat.org/data-download/
- EarthStat. Harvested Area and Yield for 175 Crops. *EarthStat.org*, Global Landscapes Initiative, University of Minnesota and Ramankutty Lab, The University of British Columbia, Vancouver. Data available online from http://www.earthstat.org/data-download/
- FAO. FAOSTAT. Available from http://faostat3.fao.org/home/E
- FAO. FAO/INFOODS Food Composition Databases. Available from http://www.fao.org/infoods/info
- Klein, A.M., Vaissiere, B.E., Cane, J.H., Steffan-Dewenter, I., Cunningham, S.A., Kremen, C., and Tscharntke, T. (2007). Importance of Pollinators in Changing Landscapes for World Crops. *Proceedings of the Royal Society B Biological Sciences* **274**:303-313. doi: 10.1098/rspb.2006.3721
- Monfreda, C., Ramankutty, N., and Foley, J.A. (2008). Farming the Planet: 2. Geographic Distribution of Crop Areas, Yields, Physiological Types, and Net Primary Production in the Year 2000. *Global Biogeochemical Cycles* **22**. doi: 10.1029/2007GB002947
- Ramankutty, N., Evan, A.T., Monfreda, C. and Foley, J.A., 2008. Farming the Planet: 1. Geographic Distribution of Global Agricultural Lands in the Year 2000. *Global Biogeochemical Cycles* **22.** doi:10.1029/2007GB002952
- USDA Nutrient Data Laboratory. USDA National Nutrient Database for Standard Reference (Release 28, released September 2015, slightly revised May 2016). Available from http://ndb.nal.usda.gov/ (accessed July 2016).
- WHO. (2009). Global Prevalence of Vitamin A Deficiency in Populations at Risk 1995–2005. WHO Global Database on Vitamin A Deficiency. WHO, Geneva, Switzerland.

4.2 Total annual excess nitrogen application

To estimate the total global excess nitrogen loads from source watersheds we use Global Nitrogen Balance dataset from West et al. (2014) at a five-minute arc grid (~10 square kilometers) resolution. We summed pixel-level nitrogen balance values for each of the Level 5 HydroBASIN units intersecting source watersheds. Polygons with positive nitrogen balances were summed to estimate total global potential excess nitrogen loading into adjacent waterbodies (~38 megatonnes). HydroBASINS with N-deficits or balanced N-budgets were not included in this global estimation.

The Global Nitrogen Balance dataset is derived from varying administrative unit detail (e.g. regional, state, country levels). In general, estimates in this dataset are more accurate in areas with high quality census data, and less in less-developed regions. The confidence level also varies by the area of aggregation.

References

- EarthStat. Total Fertilizer Balance for 140 Crops. EarthStat.org, Global Landscapes Initiative, University of Minnesota and Ramankutty Lab, The University of British Columbia, Vancouver. Data available online from http://www.earthstat.org/data-download/
- West, P.C., Gerber, J.S., Engstrom, P.M., Mueller, N.D., Brauman, K.A., Carlson, K.M., Cassidy, E.S., Johnston, M., MacDonald, G.K., Ray, D.K., and Siebert, S. (2014). Leverage Points for Improving Global Food Security and the Environment. *Science* **345**: 325-328. doi: 10.1126/science.1246067

5 Additional Data

5.1 Proportion of unprotected natural land cover within source watersheds needed to meet Aichi Biodiversity Target 11

We took a country-level approach to evaluate how source water protection activities could help to achieve the Convention on Biodiversity's Aichi Biodiversity Target 11, which states that at least 17 percent of terrestrial and inland water areas should be conserved through managed protected areas (PAs) by the year 2020.

The following statistics were calculated:

- The area and percent of each country that is protected
- The PA area and percent deficit of those countries that do not meet Aichi Biodiversity Target 11
- The area of natural land cover in source watersheds but outside of existing PAs
- Natural land cover as a percent of the protection deficit
- The percent of PAs that fall within source watersheds

PA data were gathered from the 2016 World Database on Protected Areas (WDPA) (IUCN and UNEP-WCMC 2016) produced by United Nations Environment Programme World Conservation Monitoring Centre (UNEP-WCMC) in collaboration with International Union for Conservation of Nature (IUCN). It is the largest global protected areas dataset, including both marine and terrestrial PAs. Because the 17-percent target addresses protection of terrestrial and inland water areas specifically, we excluded marine and coastal areas from the analysis. PAs falling into all management categories and all designations were used. Some PA location data were provided as points rather than polygons, and we included those with size information in the analysis by creating a circular buffer around the points. This approach follows that outlined by the Biodiversity Indicators Partnership (www.bipindicators.net) for measuring progress toward Aichi Target 11.

To calculate the percent area of each country that is under protection, all protected areas were converted to a raster grid with a 150-meter by 150-meter cell size. Protected areas smaller than a single cell (0.0225 square kilometer) were excluded from the analysis. Globally, this resulted in the loss of 296 square kilometers, or 0.0006 percent of PAs. The area of all PAs was summed for each country. Then the percent and area deficit were calculated for those countries that did not meet the 17 percent protection target.

Next, we evaluated whether the protection of natural land within source watersheds could help countries overcome their PA deficit. Data for natural land came from the 2009 GlobCover project's global land cover dataset (ESA and UCL 2009). We identified land-cover classes that are considered predominantly natural by excluding cropland and urban areas. The area of natural land within watersheds but outside of already existing PAs was summed. Then natural area as a percentage of total additional area required to reach the Aichi Biodiversity Target 11 was calculated to determine which countries could reach the target with targeted land protection as a source water protection activity. As it is unrealistic that source water protection would protect 100 percent of natural land within source watersheds, we also calculated how many countries could meet the target if 10 percent, 25 percent and 50 percent of natural land within each country's source watershed area were protected.

Inaccuracies in the results may stem from the original WDPA dataset, such as misreporting of information by providers or complete lack of size information for PA points, preventing such

PAs from being included in the analysis all together. Additionally, incorporating point data into the analysis can give rise to errors given the incorrect shape of the points' buffers. Buffers that hug country or regional boundary lines may be incorrectly distributed between them. Or, where buffers overlap with other PA polygons, the area of overlap may be over or underestimated, affecting how much area outside of the overlap is included in the total.

References

- Arino, O., Ramos Perez, J.J., Kalogirou, V., Bontemps, S., Defourny, P., Van Bogaert, E. (2012). Global Land Cover Map for 2009 (GlobCover 2009). European Space Agency (ESA) and Universite catholique de Louvain (UCL). Available from http://due.esrin.esa.int/page_globcover.php (accessed July 2016).
- Bontemps, S., Defourney, P., Van Bogaert, E., Arino, O., Kalogirou, V., and Ramos Perez, J.J. (2011). GLOBCOVER 2009: Products Description and Validation Report. Available from http://due.esrin.esa.int/files/GLOBCOVER2009 Validation Report 2.2.pdf
- IUCN and UNEP-WCMC. (2016). World Database on Protected Areas (WDPA) [Online]. UNEP-WCMC, Cambridge, UK. Available from https://www.protectedplanet.net/ (accessed July 2016).
- UNEP-WCMC. (2016). World Database on Protected Areas User Manual 1.3. UNEP-WCMC, Cambridge, UK. Available from http://wcmc.io/WDPA_Manual.

5.2 Reducing regional species extinction risk

To assess the potential avoidance of extinctions (potential species savings) due to reforestation and restoration opportunities, we first quantified the number of species within each of 804 terrestrial ecoregions for three taxonomic groups (terrestrial mammals, amphibians and birds). Spatial data for all species ranges were obtained from the IUCN Red List of Threatened Species assessment (BirdLife International and NatureServe 2015; IUCN 2016).

Next, we obtained spatial data for global forest landscape restoration opportunities (Minnemeyer et al. 2011) from WRI's Atlas of Forest Landscape Restoration Opportunities (WRI 2014). Only wide-scale and remote restoration opportunities were used in this analysis (hereafter collectively referred to as "reforestation opportunities"). Mosaic restoration opportunities were removed from the analysis because they are located in more densely populated regions and were defined in such a way that they are suitable places for multiple land uses, including agroforestry, smallholder agriculture and settlements. Any of the reforestation and restoration opportunities that were not located within the boundaries of the urban source watersheds were removed from the analysis.

To measure the change in land-use mix before and after implementing potential reforestation and restoration opportunities, we used a global map of land-use types (approximately 1 x 1 kilometers resolution) for the year 2005 (Hoskins et al. 2015). This data set was generated through the statistical downscaling of the Land-Use Harmonization dataset (Hurtt et al. 2011). Five different land-use types were considered: 1) primary habitat; 2) secondary habitat; 3) pasture; 4) crop; and 5) urban. We first calculated the area of each land-use type within each ecoregion prior to reforestation activities (i.e., current land-use mix). Next, we converted locations of reforestation and restoration opportunities to primary habitat and recalculated the area of each land-use type within each terrestrial ecoregion (i.e., future land-use mix). In the event that the wide-scale and remote reforestation opportunities overlapped with land-use pixels of cropland or urban land use, we did not apply any conversion of land use to primary

habitat. Thus, it was assumed that only the areas of secondary habitat and pasture could be restored and converted to primary habitat.

For predicting species extinctions due to human land use within a region, models describing species—area relationships (SARs) have often been employed. Recent studies have shown that a countryside SAR model outperforms other forms of SARs in predicting extinctions in heterogeneous landscapes (Pereira et al. 2014). Unlike classic SAR, countryside SAR accounts for the fact that species adapted to human-modified habitats also survive in the absence of their natural habitat (Pereira et al. 2014).

Using the current land-use mix, the SARs project the number of species expected to go extinct compared to those occurring naturally prior to human intervention in a region (Wearn et al. 2012). Note that SARs only provide an estimate of final, equilibrium level of species loss but do not tell which particular species will go extinct. Following land-use changes or habitat degradation, species do not go extinct immediately. Instead, a process of time-delayed community "relaxation" usually occurs, where species progressively disappear over time (Brooks et al. 1999). This time delay offers a window of conservation opportunity, during which it is possible to restore habitat or implement alternative measures such as reforestation to safeguard the persistence of species that are otherwise committed to extinction.

In order to calculate potential species savings due to reforestation activities, we subtracted the total species extinctions projected by countryside SAR using the future land-use mix $(S_{lost,g,j}^{future})$ from those projected using current land-use mix $(S_{lost,g,j}^{current})$.

Countryside SAR projects the total species loss $(S_{lost,g,j})$ per taxonomic group g due to current land-use mix in an ecoregion j by (for details see Chaudhary et al. 2015).

$$S_{lost,g,j}^{current} = S_{org,g,j} - S_{org,g,j} * \left(\frac{A_{new,j}^{current} + \sum_{i=1}^{n} h_{g,i,j} \cdot A_{i,j}^{current}}{A_{org,j}} \right)^{z_{j}}$$

$$(1)$$

where $S_{org,g,j}$ is the original number of species occurring in the original natural forest area $A_{org,j}$, $A_{new,j}$ is the remaining natural (primary) habitat area in the region, $A_{i,j}$ is the current area of land-use type i, $h_{g,i,j}$ is the affinity of the taxonomic group to the land-use type i and z_j is the exponent for the SAR model. If the converted land-use type is completely hostile and cannot host any species of the taxon, the h_i value equals to 0. On the other hand, if the converted land use is as benign as the natural undisturbed habitat, $h_i = 1$ (Pereira et al. 2014). This equation provides projected regional extinctions, producing the number of species expected to go extinct from a particular ecoregion only.

Next, the number of projected extinctions given the future land-use mix (i.e., once all areas identified with reforestation opportunities have been converted to primary forests) is given by:

$$S_{lost,g,j}^{future} = S_{org,g,j} - S_{org,g,j} * \left(\frac{A_{new,j}^{future} + \sum_{i=1}^{n} h_{g,i,j} \cdot A_{i,j}^{future}}{A_{org,j}}\right)^{z_{j}}$$

$$(2)$$

Finally, the potential species savings are calculated as:

$$S_{savings,g,j} = S_{lost,g,j}^{current} - S_{lost,g,j}^{future}$$
(3)

References

- BirdLife International and NatureServe. (2015). Bird Species Distribution Maps of the World. Version 5.0. BirdLife International, Cambridge, UK and NatureServe, Arlington, USA.
- Brooks, T.M., Pimm, S.L., and Oyugi, J.O. (1999). Time Lag Between Deforestation and Bird Extinction in Tropical Forest Fragments. *Conservation Biology* **13**: 1140-1150. doi: 10.1046/j.1523-1739.1999.98341.x
- Chaudhary, A., Verones, F., de Baan, L., and Hellweg, S. (2015). Quantifying Land Use Impacts on Biodiversity: Combining Species—Area Models and Vulnerability Indicators. *Environmental Science & Technology* **49**: 9987-9995. doi: 10.1021/acs.est.5b02507
- Drakare, S., Lennon, J.J., and Hillebrand, H. (2006). The Imprint of the Geographical, Evolutionary and Ecological Context on Species—Area Relationships. *Ecology Letters* **9**: 215-227. doi: 10.1111/j.1461-0248.2005.00848.x
- Hoskins, A.J., Bush, A., Gilmore, J., Harwood, T., Hudson, L.N., Ware, C., Williams, K.J., and Ferrier, S. (2016). Downscaling Land-Use Data to Provide Global 30" Estimates of Five Land-Use Classes. *Ecology and Evolution* **6**: 3040-3055. doi: 10.1002/ece3.2104
- Hurtt, G.C., Chini, L.P., Frolking, S., et al., (2011). Harmonization of Land-Use Scenarios for the Period 1500–2100: 600 Years of Global Gridded Annual Land-Use Transitions, Wood Harvest, and Resulting Secondary Lands. *Climatic Change* **109**: 117-161. doi: 10.1007/s10584-011-0153-2
- IUCN 2016. The IUCN Red List of Threatened Species. Version 2016-2. Available from http://www.iucnredlist.org (accessed July 2016).
- Minnemeyer, S., Laestadius, L., Sizer, N., Saint-Laurent, C., and Potapov, P. (2011). A World of Opportunity for Forest and Landscape Restoration. Brochure for *Atlas of Forest and Landscape Restoration Opportunities*. World Resources Institute. Washington, D.C., USA. Available from http://www.wri.org/sites/default/files/world of opportunity brochure 2011-09.pdf. Also see www.wri.org/forest-restoration-atlas (accessed September 2016)
- Pereira, H.M., Ziv, G., and Miranda, M. (2014). Countryside Species-Area Relationship as a Valid Alternative to the Matrix-Calibrated Species-Area Model. *Conservation Biology* **28**: 874-876. doi: 10.1111/cobi.12289
- Wearn, O.R., Reuman, D.C., and Ewers, R.M. (2012). Extinction Debt and Windows of Conservation Opportunity in the Brazilian Amazon. *Science* **337**: 228-232. doi: 10.1126/science.1219013
- WRI. (2014). Atlas of Forest Landscape Restoration Opportunities. World Resources Institute, Washington, D.C., USA. Available from www.wri.org/forest-restoration-atlas.

5.3 Rarity-weighted richness of freshwater and terrestrial ecoregions

Data on rarity-weighted richness (RWR) for terrestrial and freshwater ecoregions were obtained from the analysis completed by Abell et al. (2010). RWR is defined by the number of species in a given ecoregion, weighting each species by the inverse of the number of different ecoregions it occupies. Thus, the RWR measure considers two common metrics of biodiversity importance: 1) the number of unique species; and 2) the rarity of each species based on the extent of its range (Abell et al. 2010). For both terrestrial and freshwater ecoregions, highest biodiversity values are in the first quartile and lowest are in the fourth.

Reference

Abell, R., Thieme, M., Ricketts, T. H., Olwero, N., Ng, R., Petry, P., Dinerstein, E., Revenga, C., and Hoekstra, J. (2011). Concordance of Freshwater and Terrestrial Biodiversity. *Conservation Letters* **4**: 127–136. doi:10.1111/j.1755-263X.2010.00153.x

Water Funds Explorer

Table 2.1. Definitions of the main categories of source water protection activities undertaken by a given water fund, as reported by that water fund's program manager(s).

Source water	
protection activit	ty

Description



Targeted land protection. Protecting targeted ecosystems, such as forests, grasslands or wetlands.



Revegetation. Restoring natural forest, grassland or other habitat through planting (direct seeding) or by enabling natural regeneration; includes pastureland reforestation.



Riparian restoration. Restoring natural habitat that is at the interface between land and water along the banks of a river or stream. These strips are sometimes referred to as riparian buffers.



Agricultural best management practices (BMPs). Changing agricultural land management to achieve multiple positive environmental outcomes.



Ranching best management practices (BMPs). Changing land management practices on ranchlands to achieve multiple positive environmental outcomes.



Fire risk management. Deploying management activities that reduce forest fuels and thereby reduce the risk of catastrophic fire.

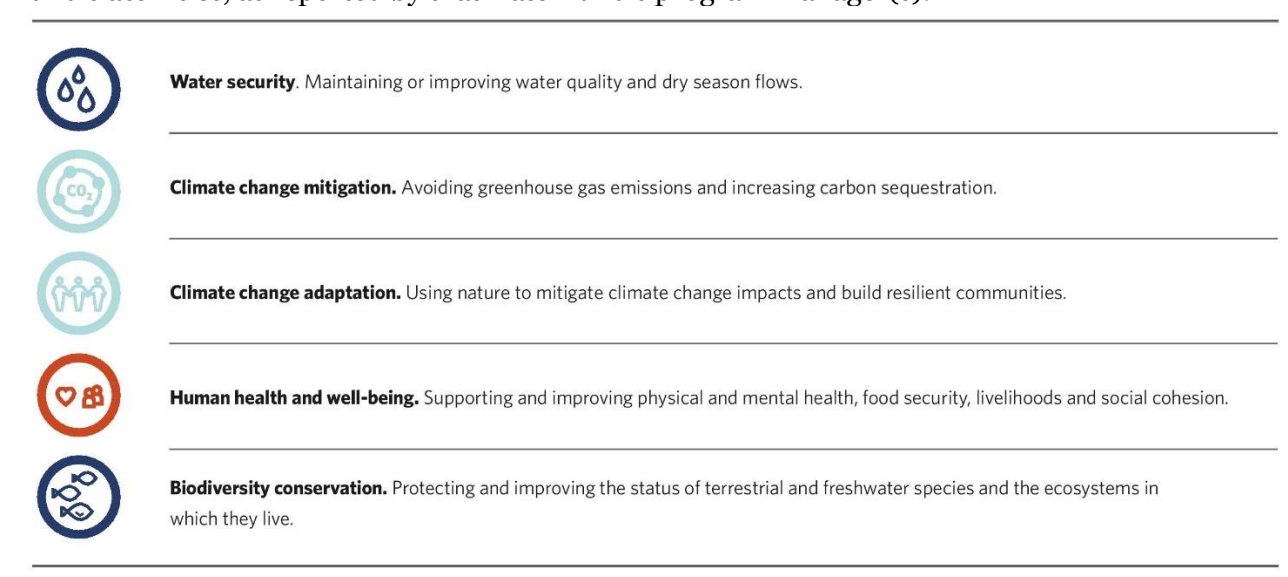


Wetland restoration and creation. Re-establishing the hydrology, plants and soils of former or degraded wetlands that have been drained, farmed or otherwise modified, or installing a new wetland to offset wetland losses or mimic natural wetland functions.



Road management. Deploying a range of avoidance and mitigation techniques that aim to reduce the environmental impacts of roads, including those impacts related to negative effects on soils, water, species and habitats.

Table 2.2. Definitions of the main categories of benefits anticipated as a result of a given water fund's activities, as reported by that water fund's program manager(s).



Water Scarcity Explorer – Data and Methods

The balance of water supply and demand within each of the world's water basins has been assessed by numerous research groups, using a variety of global hydrology models. Model outputs from the newest version of "Water A Global Assessment and Prognosis" (referred to as the WaterGAP3 model)¹ have been used in the Water Share report² as the basis for understanding where water scarcity exists around the globe and how water is being used in each water basin.

WaterGAP3 calculates water balance outputs for 143,653 individual water basins globally. Following the approach taken by Brauman and others³ for data reliability reasons, only the 15,084 of these water basins larger than 1,000 square kilometers, constituting 90 percent of total land area, are used in developing conclusions and recommendations.^{2,4}

1 Time Series of irrigation depletion

More than 90% of water consumption in water-scarce regions goes to irrigated agriculture5, but we were interested in looking at the growth of that over consumption. Using data from WaterGAP3³ and historical data derived at decadal scale from Siebert el al⁶ we created a time series of water depleted by irrigation from 1900 to 2000. Using the area under irrigation in 10-year time stamps, we calculated a ratio of area under irrigation to available water which was then iterated over the historical time series. Once each WaterGAP basin had 10 values (one per decade in the 20th century) the same algorithm that produced the categories in WaterGAP was used to define these values in terms of depletion categories.

2 Water Scarcity Condition Categories

In order to derive the categories (which we provide recommendations for in our report) we calculated the leading sector of water use for every WaterGAP3 basin in relation to its depletion level – chronic and episodic.

Chronically depleted, is when more than 75 percent of the renewable water replenishment is consumptively used on either an annual or seasonal basis. Episodically depleted, is when that consumptive use exceeds 75 percent of the renewable water replenishment only during drier years or droughts.

From there we calculated the water-use sector which constituted >80% of total consumption within a basin. For example, if >80% of the consumptive use in a Chronically depleted basin were based on irrigation this would be a C1 as outlined in our report.2 Alternatively if >80% of the consumptive use in an Episodic basin were being used by livestock, this would be an E3.

References

- 1. WaterGAP3 is an integrated water resource model developed at the University of Kassel in Germany.
- 2. Richter, B. (2016). Water Share: Using Water Markets and Impact Investment to Drive Sustainability. The Nature Conservancy, Washington, D.C., USA.
- 3. Brauman, K. A., Richter, B. D., Postel, S., Malsy, M., and Flörke, M. (2016). Water Depletion: An Improved Metric for Incorporating Seasonal and Dry-Year Water Scarcity into Water Risk Assessments. *Elementa: Science of the Anthropocene* **4**: 000083. doi: 10.12952/journal.elementa.000083

- 4. This excludes a large number of small coastal watersheds.
- 5. Wada, Y., Beek, L., and Bierkens, M.F. (2012). Nonsustainable Groundwater Sustaining Irrigation: A Global Assessment. *Water Resources Research* **48**. doi: 10.1029/2011WR010562
- 6. Siebert, S., Kummu, M., Porkka, M., Döll, P., Ramankutty, N., and Scanlon, B.R. (2015). A Global Data Set of the Extent of Irrigated Land from 1900 to 2005. *Hydrology and Earth System Sciences* 19: 1521-1545. doi:10.5194/hess-19-1521-2015